Corner Reflectors Revisited Again

Part 5: The Very-Wide-Band Corner Reflector

L. B. Cebik, W4RNL (SK)

In the course of our meanderings through the properties of corner reflectors, we have found only two driver assemblies that would expand the 2:1 SWR bandwidth to slightly over 25%: the fan dipole and a pair of in-phase-fed collinear dipoles. The latter driving option required a considerable expansion of the vertical dimension--or the rod length for rod-based reflectors--to achieve its peak performance.

A standard feature of some texts that deal with corner reflectors is a UHF television receiving array with a claimed 2:1 frequency range. Developed about a half century ago, the array now receives truncated descriptions in such volumes as Kraus, *Antennas*, 2nd Ed., pp. 557-559, and Johnson (ed.) *Antenna Engineering Handbook*, 3rd Ed., pp. 29-21 to 29-24. The Johnson volume provides some of the measured data for the array, while the Kraus text supplies some interesting dimensional detail. However, the principles behind the array appear not yet to have been modeled as a means of comparing the antenna to other reflector arrays.

Obviously, the array holds considerable interest, if for no other reason than the challenge of modeling its key features. That task will be the chief effort of this fifth episode on corner reflectors. The job is subject to a number of qualifications. First, this entire series is based upon a feedpoint of 50 Ohms for builder convenience and to confine the scope of our work into a series of projects that we can compare, one with another. However, Kraus reports that the design was intended for use with a "300 or 400 Ohm twin line." We shall model the driver assembly as a 50-Ohm system when placed within the confines of a 90-degree corner reflector.

Second, we have throughout used a 2:1 SWR standard as marking the edges of the operating passband when examining the band width of the arrays under scrutiny. Since the wide-band corner array of yore was designed for television reception nearly a half century ago, it is likely that a 2:1 standard was not applicable. It is more likely that some form of measure of signal strength at the television terminals, measured or calculated, provided the terms of bandwidth specification. However, in our work, we shall continue to use the 2:1 50-Ohm SWR value as marking passband limits. However, we shall also discover that even with those limits, the gain and front-to-back performance of a reflector array may extend considerably beyond the widest limits that we shall use.

Third, for practical reasons, I shall call any guidance provided by the modeling in this episode less general and more "proof-of-principle" in nature. As we shall see, my model for the driver of the array will only capture some of the essential features, enough to isolate what makes it the key element in expanding the flat-fan dipole driver passband from something over 25% to about 40%. As well, my rod reflector will also differ from the published versions, although it is close enough to replicate the essential ingredients of the original's performance. Finally, I shall by-pass the commercially appropriate procedure of designing to an upper and lower frequency limit, with a resultant mid-frequency. Instead, as with all of the other arrays in this series, I shall design the model for near resonance at 299.7925 MHz, so that 1 wavelength at the design frequency will equal 1 meter. Then, we shall discover where the passband will end in each direction and what the performance will be across the range of frequencies between those limits.

Let's begin by seeing what the consequence of those changes might be. The passband that we shall encounter will be shaped just like the ones that we have so far reviewed, with a steeper curve below the design frequency than above it. Hence, a true design mid-frequency will be significantly above our design frequency, about 8.3% to be more precise (325 MHz). Let's survey the dimensional results of these numbers. The "Kraus" column uses mid-frequency values derived from Kraus' description. The "Design" column gives the values as a function of our 299.7925-MHz design frequency. The final "Mid-Frequency" column adjusts those values to the passband mid-frequency. All dimensions are in wavelengths,

Dimension	Kraus	Design	Mid-Frequency
Dipole-to-apex spacing	0.40	0.50	0.54
Reflector rod length	1.20	1.20	1.30
Reflector rod diameter	0.015	0.030	0.0325
Reflector rod spacing	0.092	0.10	0.108
Reflector side length	0.113	1.20	1.30

The individual reflector measurements do not create any significant problems. The slightly wider reflector rod spacing is compensated for by the much larger diameter of the modeled rods. Otherwise, the dimensions of the listed model reflector and the design reflector are quite close. However, the mid-frequency adjustment to those values suggests that we are beginning with a reflector that is overall a bit larger than the original.

The one figure that does not jive well with the listed dimensions is the spacing from the driver to the reflector apex, with a 20% to 30% difference, depending on how one counts. Reconciling that much difference requires that we take a closer look at both the original and the modeled driver. However, since the driver design is the key to the array's wide-band performance, that is just where we ought to begin anyway.

The Forward-Bent Fan Dipole

We are familiar by now with a fan dipole. We have used one with both wire-grid and rod reflectors in past episodes. What converts the standard flat fan dipole into a Brown-Woodward "bow-tie" dipole is bending the dipole down its axis so that, relative to a corner reflector, it bends forward at a 90-degree angle. **Fig. 1** shows the difference.

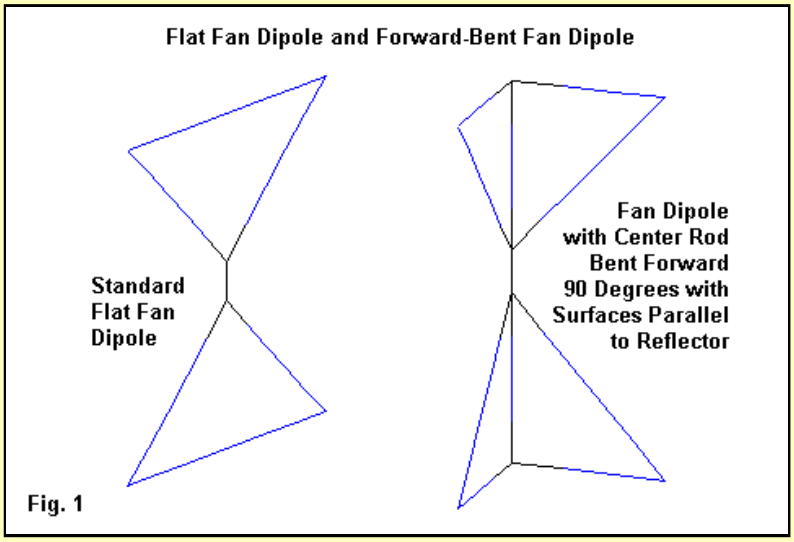

Contrary to existing literature, that describes a horizontal version of the subject array for television reception, I shall continue our convention of using a vertical orientation, in light of anticipated 21st century best uses for a corner reflector. The change of orientation is the least of the list of matters with which we need to be concerned with respect to the model. First, note the addition of an "axis" wire running from end to end. This wire alters the performance of the bent model relative to the flat design. In the flat model, the terminating point is always at the exact center of each wire end between the tips of the triangle. With a center wire added, the end point may shift somewhat.

The bent fan dipole requires some dimensional adjustment to align it with the flat fan. The side-to-side dimension, as measured from the centerline to a tip, shrinks from 0.11 wavelength to 0.108 wavelength. However, the overall length of the dipole increases from 0.24 wavelength for the flat version to 0.262 wavelength for the bent version. The bends in the fan are designed so that they will be parallel to the plane of the reflector itself when finally situated.

Sketches of the Brown-Woodward (B-W) dipole show 3 differences from the modeled version. First, the angle taken by the perimeter edge is shallower in the sketches than in the model. The model approaches a 45-degree angle relative to the centerline, while sketches give no clear indication of the B-W angle. The smaller angle of the sketched design may account for the fact that its listed mid-frequency length is 0.8 wavelength, rather than the 0.242- wavelength value of the model at the design frequency. Second, sketches seem to indicate that instead of a sharp bend, such as used in the sketch, there may be a flat area along the center line, with bends beginning at some point away from the centerline. Third, the B-W bow tie is a solid sheet. The model is a set of perimeter wires. However, the wire is the same 8-mm diameter wire used for the flat fan. Hence, some of the effect of the actual flat area may be captured by the wire diameter along the centerline of the antenna, while the wire thickness may capture something of the solid surface.

Nevertheless, the differences are enough to make the notes on the very-wide-band corner array less than useful for general design guidance. At most, they may serve to prove the principle of using a forward-bent dipole as a driver for the corner reflector. As well, the bends in the dipole create a rise in the average gain test value for the new driver. Because we shall work within a 2:1 SWR range, we may apply a corrective to all gain values that we derive from the models (about -0.67 dB) to arrive at more accurate values. Even with all of these cautions and precautions, we shall not be able to see what gives the forward-bent fan dipole its advantage in the corner reflector by examining the driver alone.

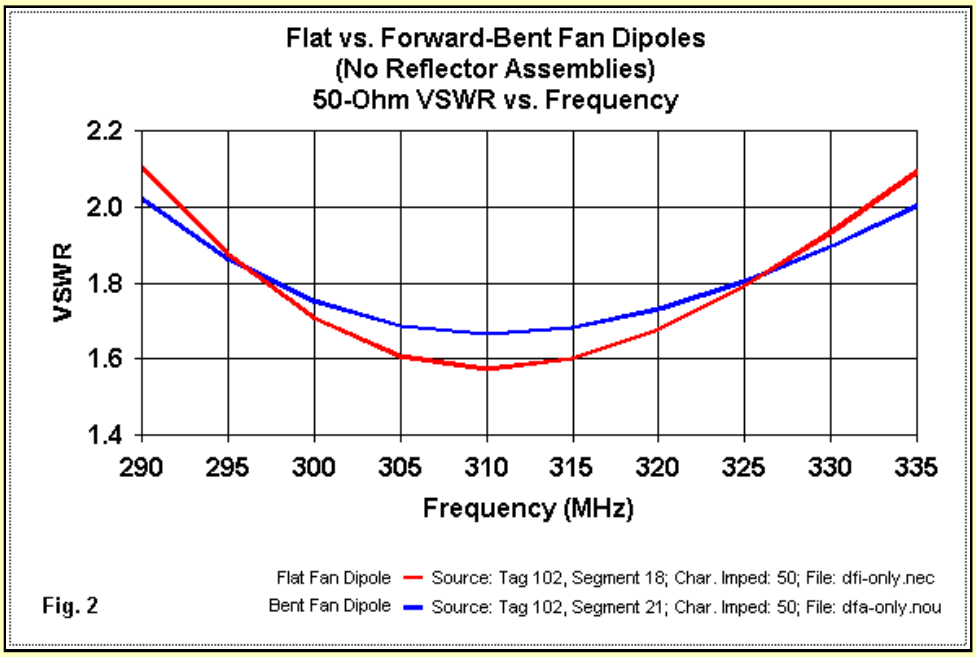

Fig. 2

As the comparative SWR graph shows, the forward-bent dipole shows only a small advantage over the flat fan dipole. Both have a resonant impedance between 28 and 30 Ohms. The comparative 50-Ohm passband are 13.3% for the flat version and 14.7% for the bent version.

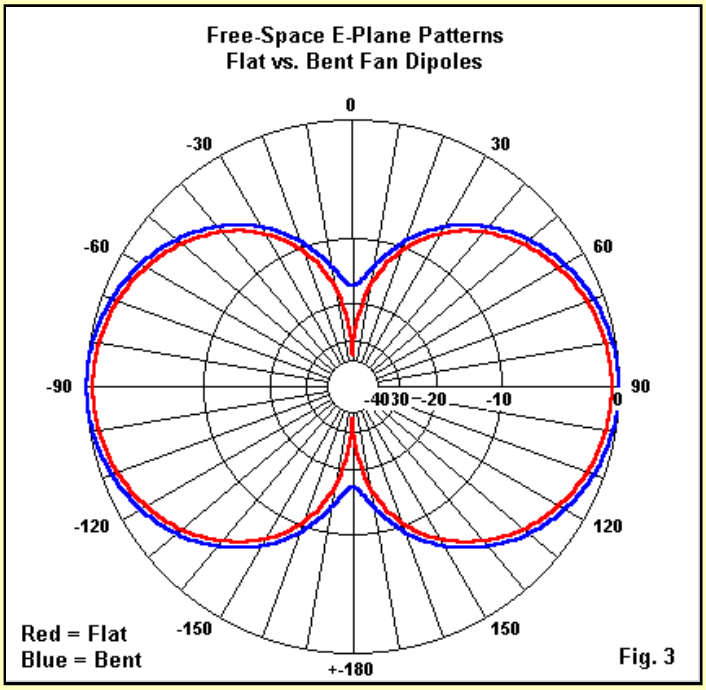

Fig. 3

Fig. 3 gives us the E-plane patterns of a flat fan and a bent fan. (The H-plane patterns of these dipoles in isolation are circles in both cases.) First, ignore the relative strengths of the patterns. It is the shape that interests us here. The flat fan shows the deep side nulls that we expect of a dipole. However, the bent dipole side-nulls do not reach 20 dB. This feature will reappear in a modified way when we finally reach the forward-bent fan dipole driven corner array.

The shallow depth of the bent fan side nulls is a clue to the error in the pattern graph, since both dipoles have identical drive levels. The flat fan should show a peak gain slightly greater than the peak gain for the bent version. The reason that these values are reversed is that the polar plot uses uncorrected gain values. The flat fan free-space gain varies from 2.04 to 2.16 dBi from 290 to 335 MHz. The bent fan gain varies (when corrected) from 1.84 to 1.93 dBi, an accurate reflection of the increased power off the ends of the antenna.

Perhaps the most notable fact that we have gleaned from our preliminary look at the flat and bent fans in isolation is the difference in the pattern shape in the E-plane (parallel to the axis of the antenna). For any further insights into why one might want to use a B-W dipole in a corner array, we shall have to model the driver in its working position.

The Very-Wide-Band Corner Reflector Array

When we place the drivers into their places within a corner array, the result resembles the pair of sketches shown in **Fig. 4**.

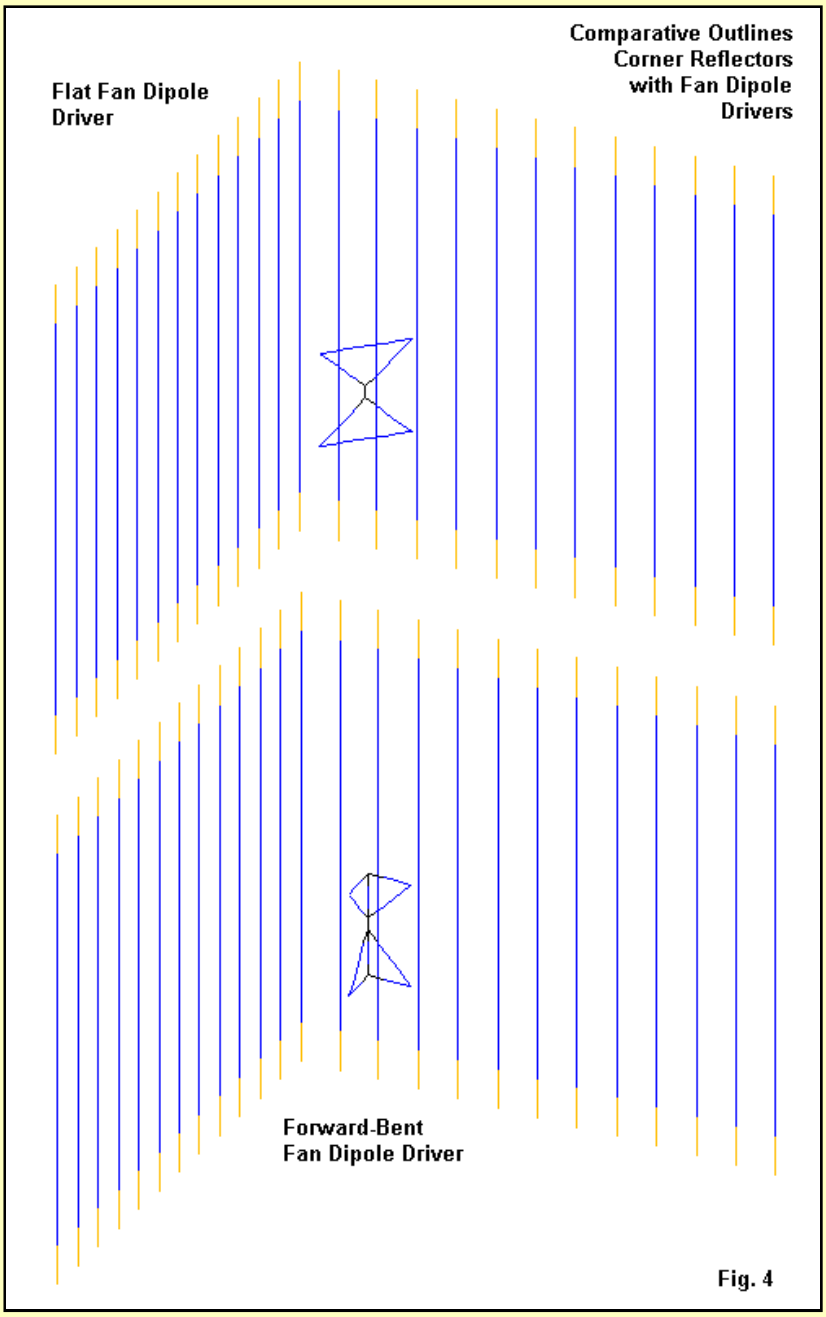

In both cases, the reflector is 1.2-m (wavelengths) vertically, and the side length is also 1.2 m (wavelengths). The flat fan is 0.49 m (wavelength) away from the reflector apex, while the centerline of the bent fan is 0.5 m (wavelength) distant from the same point. The following lines present a complete model of the bent fan driver and its rod reflector. If you wish to replicate the flat fan model, simply extract the driver geometry lines from a past episode's model and replace the bent fan rod geometry with them. The model that follows is set up for a complete frequency sweep.

```
CM Bent fan dipole-12-12-rods
CE
GW 1 12 0 0 -.6 0 0 .6 .015
GW 2 12 0 -.1 -.6 0 -.1 .6 .015
GM 0 11 0 0 0 0 -.1 0 2 1 2 12
GM 0 0 0 0 45 0 0 0 2 1 0 0
GW 3 12 0 .1 -.6 0 .1 .6 .015
GM 0 11 0 0 0 0 .1 0 3 1 3 12
GM 0 0 0 0 -45 0 0 0 3 1 0 0
GW 101 5 .57778 .075 -.131 .5 0 -.015 .004
GW 101 5 .57778 -.075 -.131 .5 0 -.015 .004
GW 101 3 .57778 .075 -.131 .5 0 -.131 .004
GW 101 3 .5 0 -.131 .57778 -.075 -.131 .004
GW 101 4 .5 0 -.131 .5 0 -.015 .004
GW 102 1 .5 0 -.015 .5 0 .015 .004
GW 103 5 .5 0 .015 .57778 .075 .131 .004
GW 103 5 .5 0 .015 .57778 -.075 .131 .004
GW 103 3 .57778 .075 .131 .5 0 .131 .004
GW 103 3 .5 0 .131 .57778 -.075 .131 .004
```

```
GW 103 4 .5 0 .015 .5 0 .131 .004
GE 0 -1 0
FR 0 14 0 0 265 10
GN -1
EX 0 102 1 0 1 0
RP 0 361 1 1000 -90 0 1.00000 1.00000
FR 0 14 0 0 265 10
RP 0 1 361 1000 90 0 1.00000 1.00000
EN
```

GW entries 101 through 103 give the driver details, while the preceding lines set the reflector geometry. The FR entries that supply frequency details give away the results to come. They specify a frequency sweep from 265 to 395 MHz for the array. **Fig. 5** gives the results of that sweep for both the flat and the bent dipole drivers.

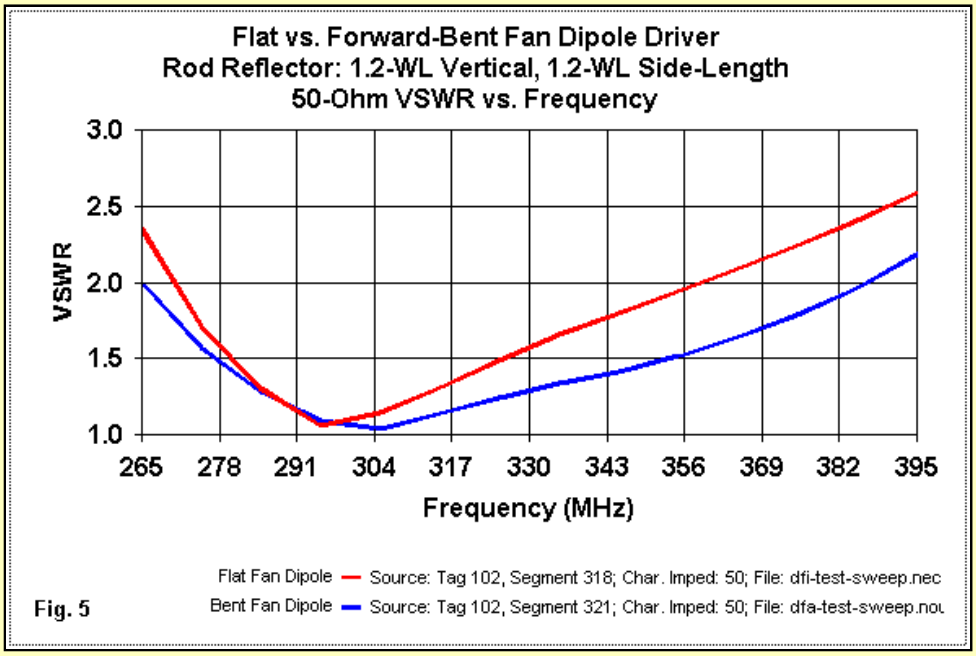

Fig. 5

For the bent dipole driver, the 2:1 SWR passband edges are 265 MHz at one end of the range and 385 MHz at the other end. This 120-MHz range is a 40% bandwidth relative to the design frequency or about 37% relative to the center-frequency of the defined passband. The bent dipole clearly provides a very significant increase in the passband relative to what a flat fan dipole can provide. According to the literature, the difference is a function of the fact that the planes of the bent fan parallel the planes of the reflector. However, that fact alone does not tell us what changes with respect to array performance. Hence, we should begin an exploration of the performance reports for the two types of drivers.

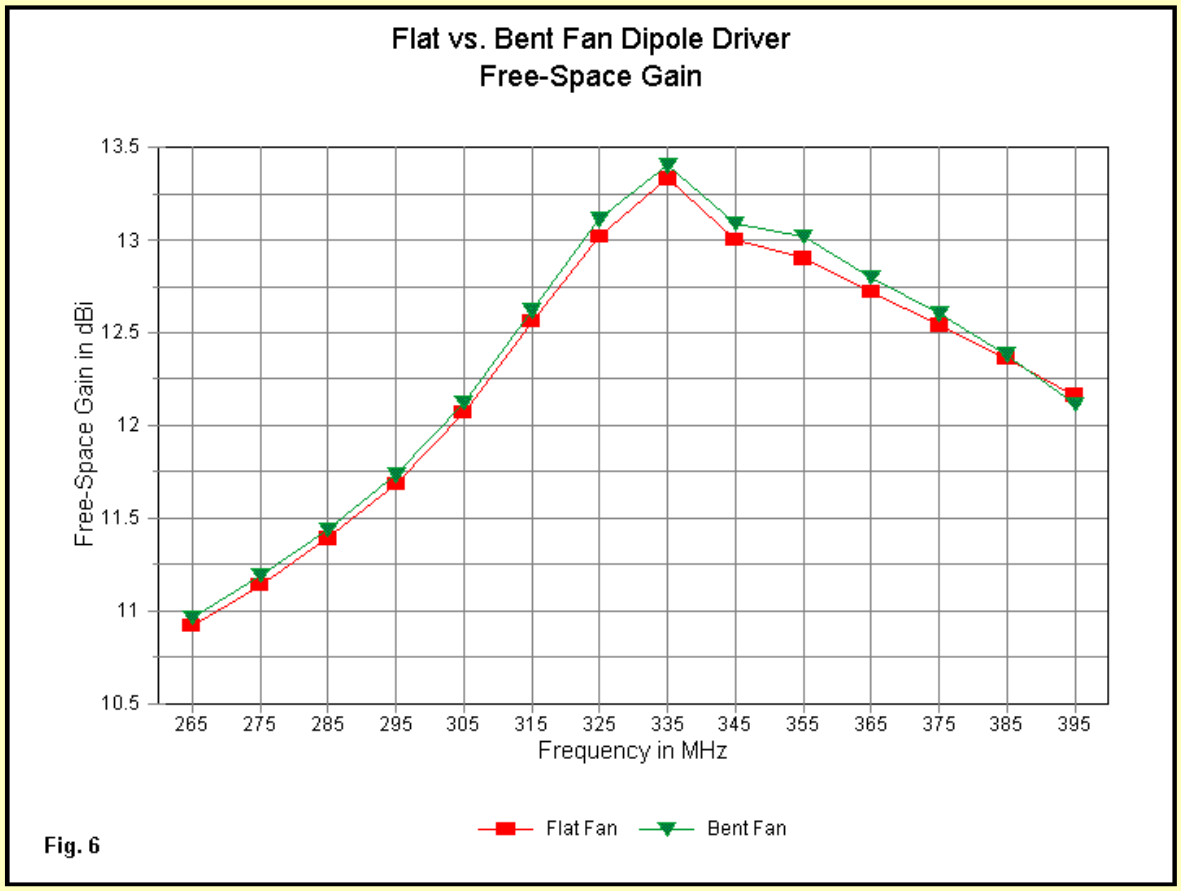

Fig. 6 gives us a comparative view of the forward gain values that we can derive from the array, using corrected values for the free-space gain. In effect, the graph tells us that there is no difference whatsoever in gain performance. Indeed, if the graph reveals anything, it is the fact that with the flat fan driver, the array performance passband extends well beyond the SWR limits set by the driver. If a 2.41-dB difference between the lowest and the highest values of gain is satisfactory for an application and if SWR is not a matter of concern, then either driver would provide the same gain service.

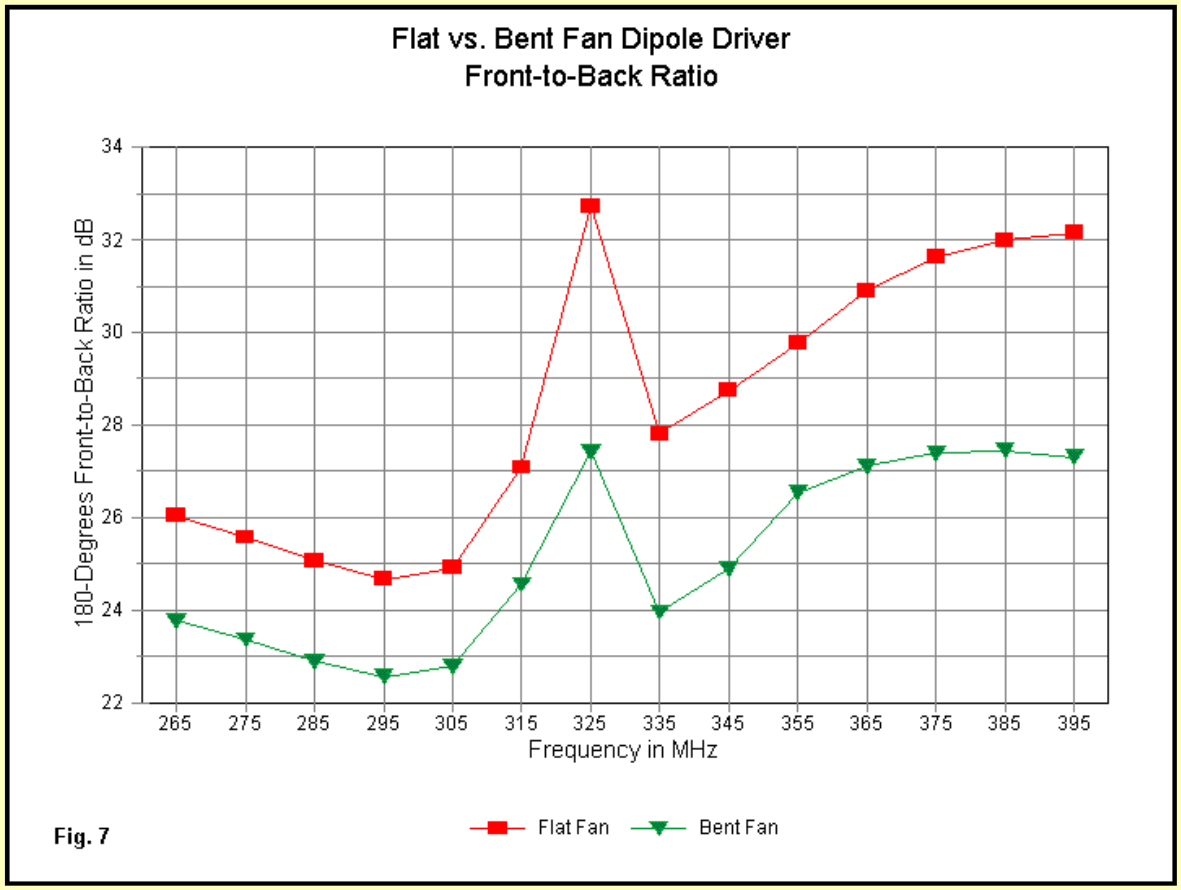

The situation is less simple when it comes to the 180-degree front-to-back ratio (**Fig. 7**). The 180-degree values, taken as a composite across the band, do reflect the overall increased rearward radiation of the bent-fan driver system. The

difference ranges from 3 to over 5 dB across the passband, and the lines are almost perfectly congruent. If we wish to probe these numbers in greater details, we must examine some patterns for the array. In the following samples, we shall find patterns in both the E-plane and the H-plane taken at the sweep extremes and at 335 MHz, the frequency of highest gain. Since the sweep extremes fall outside the SWR passband, we expect slightly weaker forward gain peaks than for the peak gain frequency.

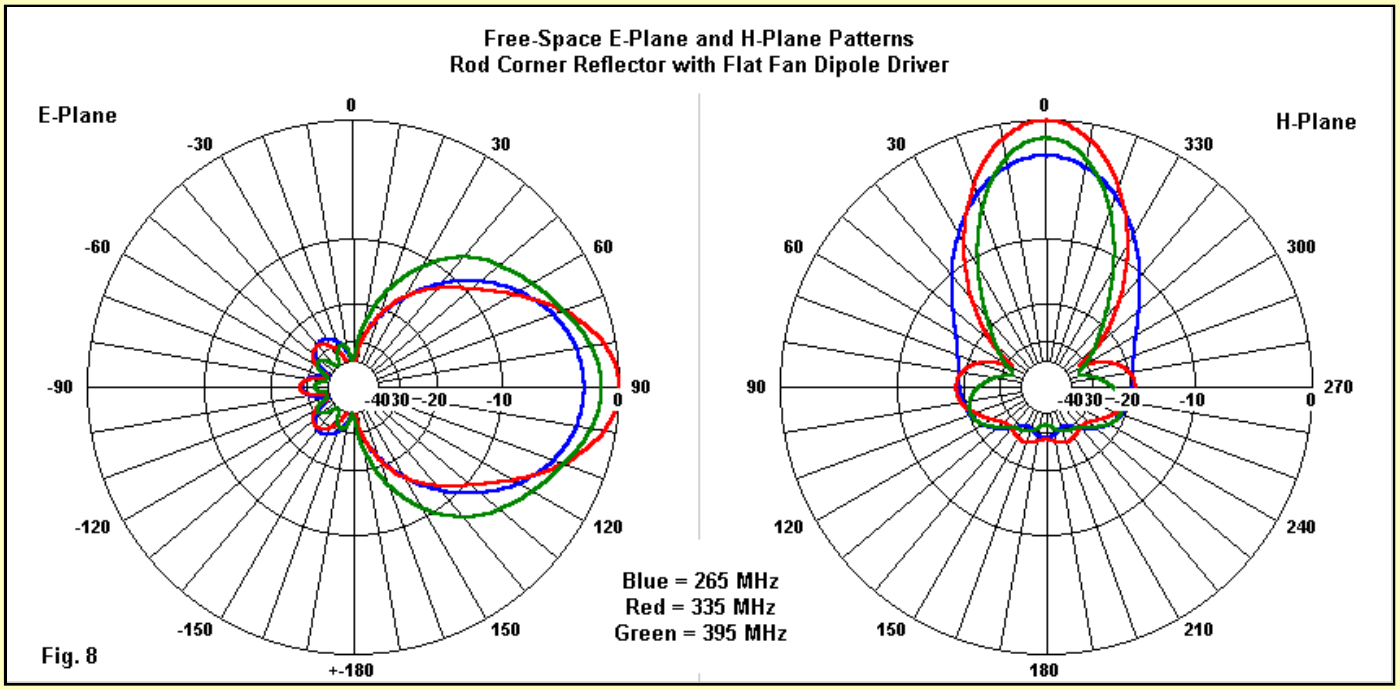

For an array with such a wide operating passband, the fat-fan patterns are quite well-behaved, as shown in **Fig. 8**. The E-plane patterns show equal half-power beamwidths at the sweep extremes--58 degrees--although the high frequency pattern has an overall broader appearance. The beamwidth shrinks to 42 degrees at the peak power frequency. Throughout the span, the rear lobes are both modest and normal, that is, well within our expectations for a high-gain array.

The H-plane patterns show more visual variation across the frequency span. The "bullet" pattern at 265 MHz evolves into a narrower forward lobe with distinct sidelobes as we move higher in frequency. By the time that we reach 300 MHz, the pattern has developed deep nulls to separate the forward lobe from two major sidelobes. These sidelobes do not change their maximum strength by much as we continue to increase frequency, even though the H-plane beamwidth shows a gradual reduction from 48 degrees at the lower end of the passband to 32 degrees at the upper end. In fact, note that the side-to-side extent of even the low-end "bullet" pattern has roughly the same strength as the sidelobes.

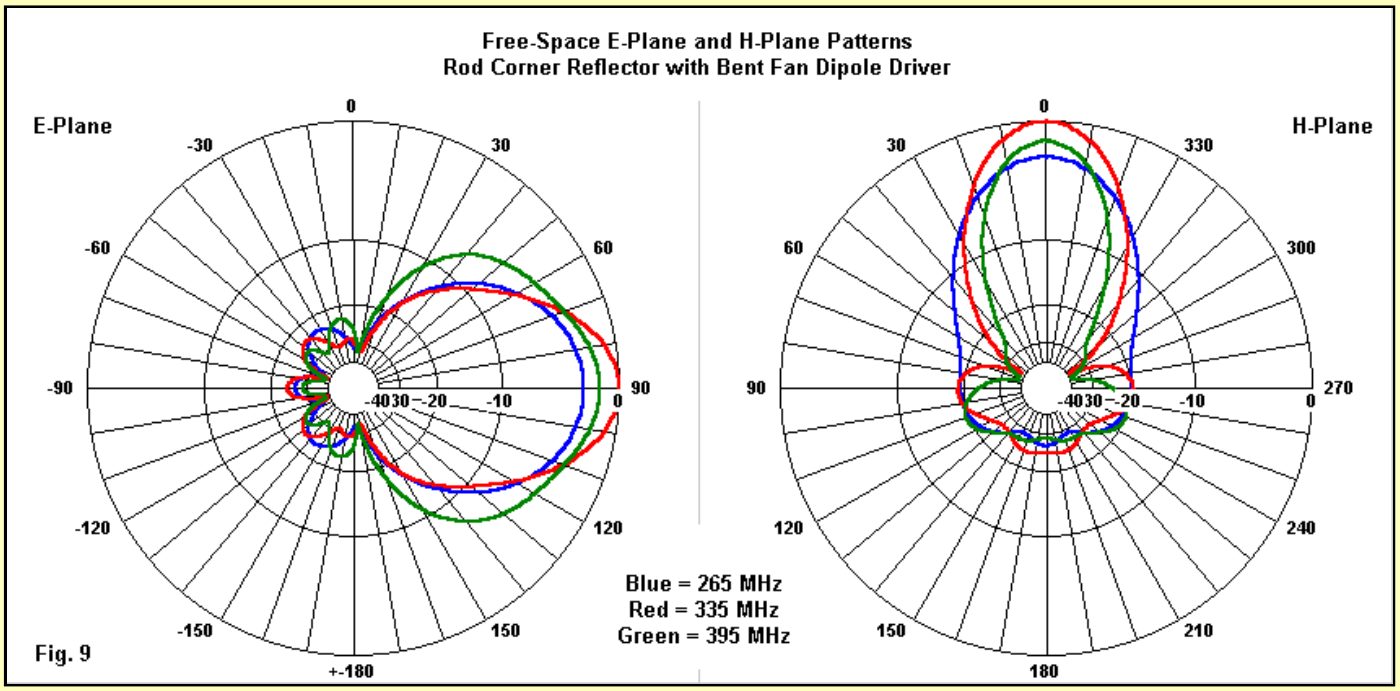

The E-plane patterns for the forward-bent fan dipole driver, shown in **Fig. 9**, are somewhat less tidy than those for the flat fan. Immediately apparent are the larger rear lobes at every sampled frequency, a fact that showed up in the front-to-back graph in **Fig. 7**. Also apparent is the wider pattern at 395 MHz with a beamwidth of 66 degrees in contrast to 58 degrees for the flat fan. However, perhaps the most notable feature is the one most easily missed. Compare the two sets of E-

plane patterns for the depth of the side nulls. The shallower side nulls for the bent fan that we first saw when looking at the antenna in isolation (**Fig. 3**) remain a part of the E-plane patterns when we use the bent fan to drive a corner reflector.

In contrast, the H-plane patterns for the bent fan are almost the same as for the flat fan. The only difference of significance is the slightly larger size of the rearward lobes or structures.

Nothing in the graphs or patterns has helped us to understand why the SWR curves for the flat and the bent fan driver systems have such different 2:1 bandwidths. The differing shapes of the drivers, including the fact that the planes of the bent fan parallel the reflector surfaces, do not create changes in the patterns that we may directly tie to the SWR level. Only one set of parameters remains to explore: the source or feedpoint impedance.

With respect to the feedpoint reactance, the very sizable difference in SWR goes unexplained. Both drivers show very normal reactance curves, beginning with a considerable capacitive reactance and ending with an equally considerable inductive reactance. There is a difference in the total reactance range: 87.02 Ohms for the flat fan and 67.28 Ohms for the bent fan. However, this difference alone does not suffice to widen the SWR bandwidth by the amount that we saw in the SWR curve in **Fig. 5**. Let's graph the respective feedpoint resistance curves and see if an answer lies there. See **Fig. 10**.

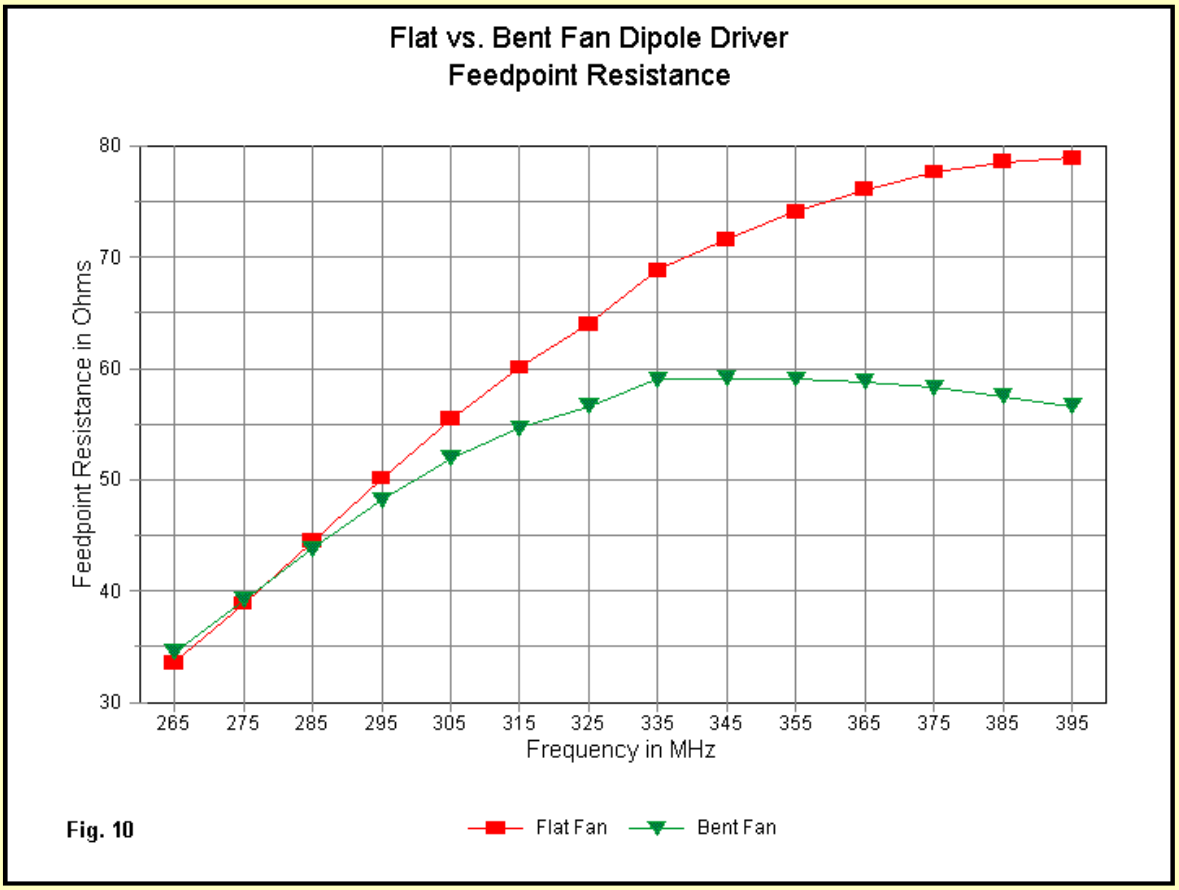

Fig. 10

The curve for the flat fan shows a very normal curve that climbs steadily upward, although it slows the rate of climb as the frequency approaches the upper limit. The bent-fan curve tells a much different tale, as it reaches a maximum value at about the same frequency as the point of highest gain. Then, as we further increase the frequency, the curve levels off and actually declines. If we re-examine **Fig. 5**, we can see that had we specified higher SWR limits of 2.5:1 or 3:1, we would have garnered considerably more territory at the high end of the band with only small increased at the low frequency end. However, note the slightly upsweep at the high end of the passband for the bent fan curve. The reactance near the upper end of the passband is increasing faster than for the flat fan system.

The mystery of the bent-fan benefit becomes somewhat clearer as we digest the resistance data. The parallel planes of the driver and the reflector likely increase coupling between the two surfaces as we increase frequency, with the normal result of a lower overall impedance in the driven element. The effect is sufficient to partially counteract the tendency toward higher impedance values with increasing frequency, at least enough to broaden the SWR bandwidth. Our little experiment--even with all of its differences from the original antenna--suffices to uncover the principle of the B-W bow-tie's prowess in serving as the focal point for a very-wide-band corner reflector. Indeed, controlling the width of the fan's projections, with consequential adjustments to its overall length, would give the designer a degree of further control over the bandwidth. In addition, one might also experiment with the angle of bend or, in other words, the level of parallelism between the driver and reflector planes as another means of controlling bandwidth.

A Brief Note on Higher Impedance B-W Bent-Fan Dipole Drivers

I have noted that the original B-W bent-fan dipole driver required 300- to 400-Ohm feedline. Physically, it is longer, end-to-end, than the 50-Ohm driver that we have used, and its spacing also differs from the value required in our modeled bent fan. Of course, the original driver used a relatively thin solid sheet, while our model used a perimeter substitute with 8-mm

diameter wire. However, something more than these differences is at work to explain the major differences in shape and length.

As an experiment, I used a 1.2-m vertical wire-grid reflector with a side length of 2.4 m, where these dimensions are also in wavelengths at the design frequency. As we shall see further on, the 50-Ohm bent fan model driver works well with such a reflector. However, my goal differed. I wanted to find out what sort of changes I would have to make to arrive at a 300-Ohm driver within the reflector.

Essentially, I had to increase the length of the driver to 0.6 m overall, more than twice the length of the 50-Ohm driver. The other driver dimensions remained unchanged. The resulting driver has a much shallower angle between the center and the ends. Using the same 8-mm wire, the shallower angles formed by the 3 joining wires on each side of the center segment reduce the adequacy of the model. As a result, the following notes are only suggestive and fall short of being a proof-of-principle model.

With a 300-Ohm design frequency impedance and very little reactance, the 2:1 SWR passband of the modified array increases from 120 MHz up to 212 MHz (with a range from about 248 MHz up to 460 MHz). In other words, the passband increases from 40% to slightly over 70%. The peak gain appears at about 440 MHz, with a corrected value of about 14.2 dBi. The position of the peak gain value tends to coincide extremely well with field measurement results reported in the Johnson volume. The gain differential across the band is about 1.9 dB.

Front-to-back values range from 23 to 32 dB. The E-plane beamwidth shows a very regular progression from 50 degrees at the low end of the scanned spectrum to 38 degrees at the upper end. By 420 MHz, the E-plane pattern shows a distinct spade shape, and at the uppermost frequency sampled, it takes on distinct side bulges, suggesting incipient secondary forward lobes.

These results strongly suggest that a B-W bent-fan dipole designed for about a 300-Ohm feedpoint impedance will further increase the operating passband of a corner array without serious performance or pattern degradation. The modeled driver shows trends in its length and shape that lean toward the sketches of the B-W driver. Nevertheless, the results are extraordinarily tentative and insufficiently reliable to be more than suggestive. The high average gain test values place the impedance values at the passband edges into some doubt, especially as the reactance levels rise to prevent corrections. As well, even the corrected gain and other performance values are subject to adjustment. Even with all of these serious qualifications and modeling limitations, the exercise gives the very-wide-band television reflector array at least a partial confirmation.

Understanding what role the B-W bent-fan dipole plays in achieving the SWR bandwidth and also discovering that it plays little role in determining the gain and front-to-back performance figures, is not only useful, but as well opens the door to further experimental work, whether conducted through modeling or field experiments--or both. The potential for an antenna using a single driver that covers a 2:1 frequency range (even at the cost of expanding SWR limits above the 2:1 value used here) has potential for a number of applications, especially above the GHz level. At those frequencies, however, one might be inclined to use solid surfaces or closely spaced screens for the reflectors. In addition, most descriptions of the very-wide-band corner reflector array note an economic and performance compromise in the setting of the reflector size. So we have at least two questions that we might pose before leaving this version of the corner reflector. 1. What do we obtain if we use large reflectors? 2. What can we expect from a reflector using a wire-grid as the modeled simulation of a solid or screened set of planes?

Bigger and Tighter Reflectors

The 1.2-m vertical by 1.2-m side-length rod reflector used to approximate the listed very-wide-band array produces good gain, but not the maximum gain of which the forward-bent fan dipole is capable. As we saw in previous episodes, there is a practical limit to the vertical dimension. Ideally, a vertical dimension (rod length) of 1.4 wavelengths yields maximum gain, but in a very-wide-band design, that dimension must occur well above the design frequency and close to the middle of the frequency range actually covered by the array. Therefore, the vertical dimension of 1.2 wavelengths appears to work best by placing the peak array gain in the middle of the passband.

Of course, the steps used for the vertical dimension are at 0.2-wavelength intervals. In the course of tests with reflectors using different vertical dimensions, the 1.4-wavlength size consistently yielded free-space gain values that peaked below the design frequency. The longer the side lengths of the reflectors, the lower the frequency of peak gain. In contrast, maintaining a vertical dimension or rod length of 1.2 wavelengths kept the peak gain value in the vicinity of 325 or 335 MHz. The resulting gain curve tends to place the lowest gain value at the low end of the passband, but sustains an appreciable gain all the way to the top of the passband.

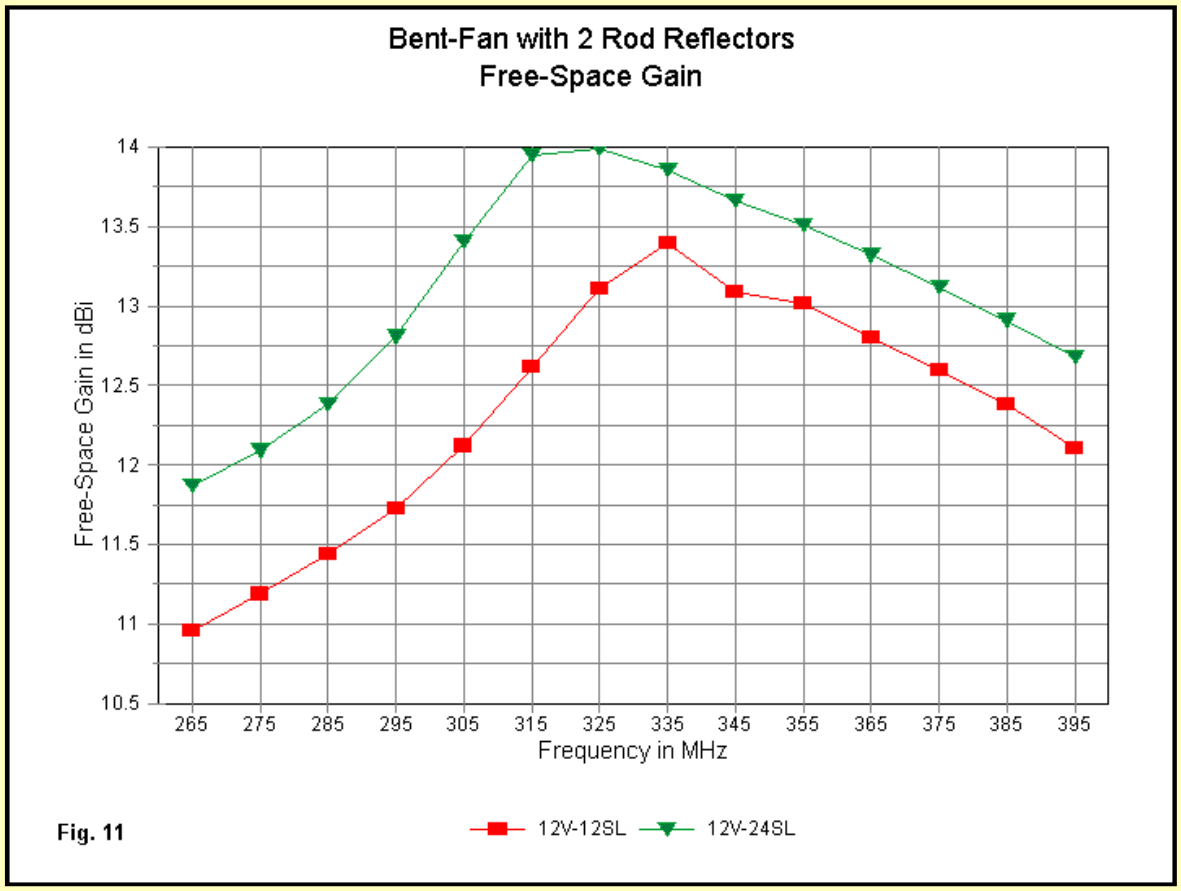

Fig. 11

Fig. 11 compares the gain levels of our initial model using a side length of 1.2 wavelengths and a second model having the same vertical dimension, but sides that are twice as long: 2.4 wavelength (as measured at the design frequency, where 1 wavelength = 1 meter). The coding on the legend indicates the vertical dimension and the side length in meters, where those values are also wavelengths at the design frequency. The peak corrected free-space gain of the expanded array is 13.99 dBi. The average gain increase across the passband--which is identical for both arrays--is about 0.67 dB. However, the larger array better centers the peak gain so that the differential from lowest to highest gain value is 2.12 dB, in contrast to the 2.41-dB differential for the smaller version of the array.

Increasing the vertical dimension to 1.4 wavelengths and retaining the new 2.4-wavelength side length produced a peak gain value of 14.08 dBi at 275 MHz. Above that frequency, the gain gradually falls off so that the top-end gain value is down to 12.15 dBi. The average gain is higher, and the differential between highest and lowest value is less: 1.93 dB. However, the lowest value for the array occurs at the highest frequency, where the E-plane beamwidth also expands to 76 degrees. For some applications, the more even forward gain value may be useful, but in most UHF applications, a rising or level gain curve is desirable.

Even at the 1.2-wavelength vertical dimension, the added gain comes at a fabrication cost that is considerable. The reflector would require a much more robust construction, whether supported behind the reflector apex or at the center of mass. In the field of UHF television reception for which the original array was designed, the lesser gain of the smaller reflector effected very good performance between 450 and 900 MHz with a practical size. Indeed, memories of UHF antenna installations suggest that the array had surplus gain, since a more common sight were planar reflectors with narrower-band drivers, one pointed at each UHF station in the region. These arrays general showed less gain by 2 to 3 dB, but provided fixed and less expensive installations. The corner array seems to have been reserved for the viewer with more funds to expend on a rotatable system.

Of course, in terms of television, all of these last notes are historical, as cable and satellite television now supply the needs of television viewers. However, the television experiences of the 1950s through the 1980s may be useful to track for anyone who may contemplate applications in the upper UHF range.

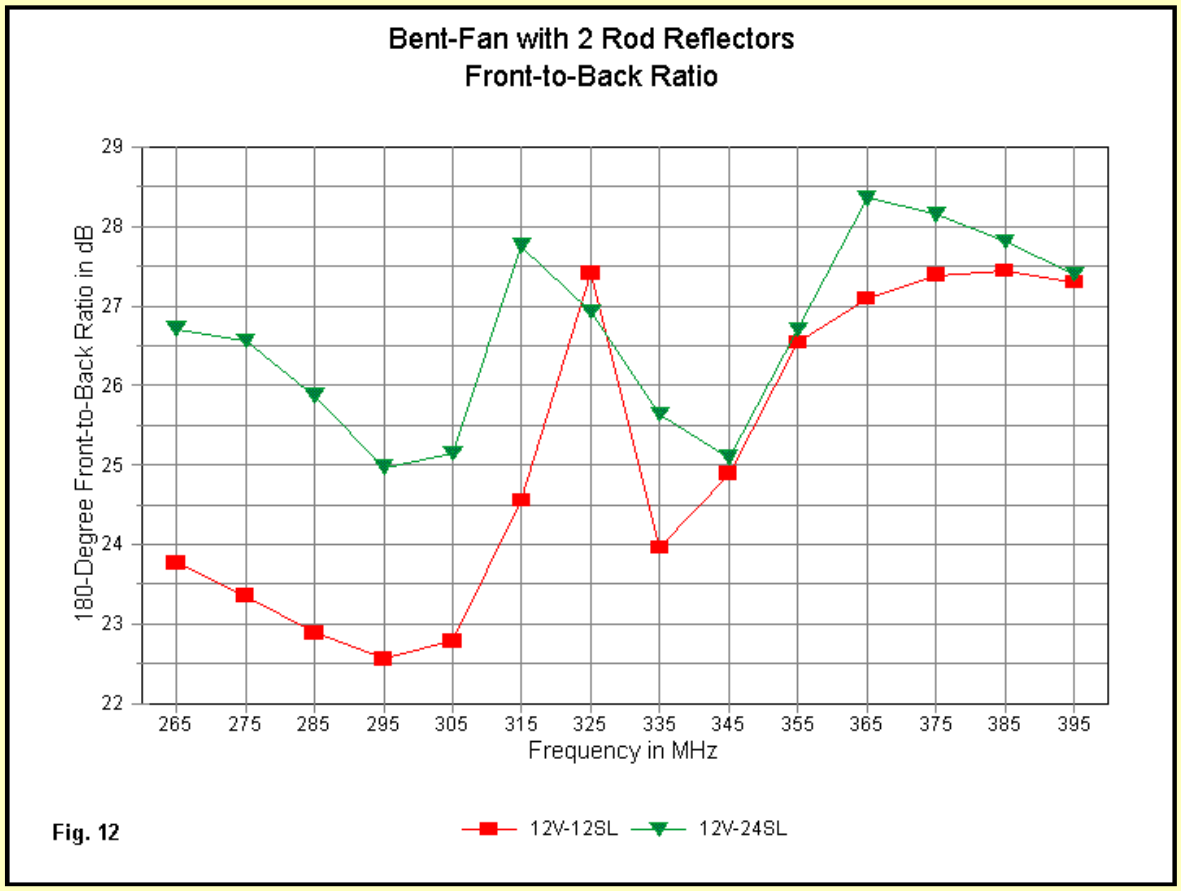

Fig. 12

The advantage of the corner reflector with longer sides in the front-to-back department is apparent from **Fig. 12**. In the lower half of the SWR passband, the longer sides provide a considerable increase in the front-to-back ratio. However, as we increase frequency and the sides grow longer as a function of a wavelength, we arrive at a limit, beyond which the front-to-back value increases no further. Using the 180-degree figure makes the task of identifying a specific frequency or even a small frequency span almost impossible. However, the graph makes it clear that for the upper half of the passband, the longer side length yields no advantage.

As we have seen in past episodes, the rod reflector has a peculiar characteristic. The gain peaks in a noticeable manner as the vertical dimension of the array reaches the vicinity of 1.4 wavelengths. If we extrapolate from the curves for the very-wide-band array curves for all of the rod reflectors using that value, it is likely that a vertical dimension of 1.30 to 1.35 wavelength may come closer to the peak gain vertical dimension. However, the exact value will vary with the rod diameter, which determines to a major degree the electrical length of the reflector rods. The physical length of our 1.4-wavelength rods would yield a significantly higher electrical length, given the 0.03-wavelength diameter. To some degree, the rod spacing will also play a role, since the spacing determines the mutual coupling between the individual rods. Although the initial theory of corner reflectors is based upon image theory, when we construct corner reflectors using rods, we cannot ignore parasitic effects that modify the results of the basic formulations.

Solid surface and closely spaced screens used as reflector surfaces showed a different set of curves as we increased both the vertical dimension and the side length of the reflector. Our model for these reflectors uses wire-grid techniques that we carefully checked in the study of planar reflectors. In general, as we increased the vertical dimension and/or the side length, we obtained smooth curves, with shallow peaks in the vicinity of a vertical dimension of 1.6-1.8 wavelength and a side length in the 2.4-2.8-wavelength region. Based on that modeling experience, I constructed a model using our forward-bent fan dipole with a 1.4-wavlength vertical dimension and a 2.4-wavelength side length at the design frequency, where these values become meters. The array size grows with increasing frequency and shrinks with decreasing frequency. The following lines provide the model used to sweep the array across the anticipated passband. As always, you may extract the model from the text, strip aways the opening and closing HTML codes, and use it directly in any version of NEC accepting .NEC-format files. You may modify the reflector size using the guidance of past episodes of this series.

```
CM Bent fan dipole-14-24-wiregrid
CE
GW 1 14 0 0 -.7 0 0 .7 .0159
GW 2 14 0 -.1 -.7 0 -.1 .7 .0159
GM 0 23 0 0 0 0 -.1 0 2 1 2 14
GW 3 24 0 0 0 0 -2.4 0 .0159
GM 0 7 0 0 0 0 0 -.1 3 1 3 24
GM 0 7 0 0 0 0 0 .1 3 1 3 24
GM 0 0 0 0 45 0 0 0 2 1 0 0
GW 4 14 0 .1 -.7 0 .1 .7 .0159
GM 0 23 0 0 0 0 .1 0 4 1 4 14
GW 5 24 0 0 0 0 2.4 0 .0159
```

```
GM 0 7 0 0 0 0 0 -.1 5 1 5 24
GM 0 7 0 0 0 0 0 .1 5 1 5 24
GM 0 0 0 0 -45 0 0 0 4 1 0 0
GW 101 5 .57778 .075 -.131 .5 0 -.015 .004
GW 101 5 .57778 -.075 -.131 .5 0 -.015 .004
GW 101 3 .57778 .075 -.131 .5 0 -.131 .004
GW 101 3 .5 0 -.131 .57778 -.075 -.131 .004
GW 101 4 .5 0 -.131 .5 0 -.015 .004
GW 102 1 .5 0 -.015 .5 0 .015 .004
GW 103 5 .5 0 .015 .57778 .075 .131 .004
GW 103 5 .5 0 .015 .57778 -.075 .131 .004
GW 103 3 .57778 .075 .131 .5 0 .131 .004
GW 103 3 .5 0 .131 .57778 -.075 .131 .004
GW 103 4 .5 0 .015 .5 0 .131 .004
GE 0 -1 0
FR 0 14 0 0 265 10
GN -1
EX 0 102 1 0 1 0
RP 0 361 1 1000 -90 0 1.00000 1.00000
FR 0 14 0 0 265 10
RP 0 1 361 1000 90 0 1.00000 1.00000
EN
```

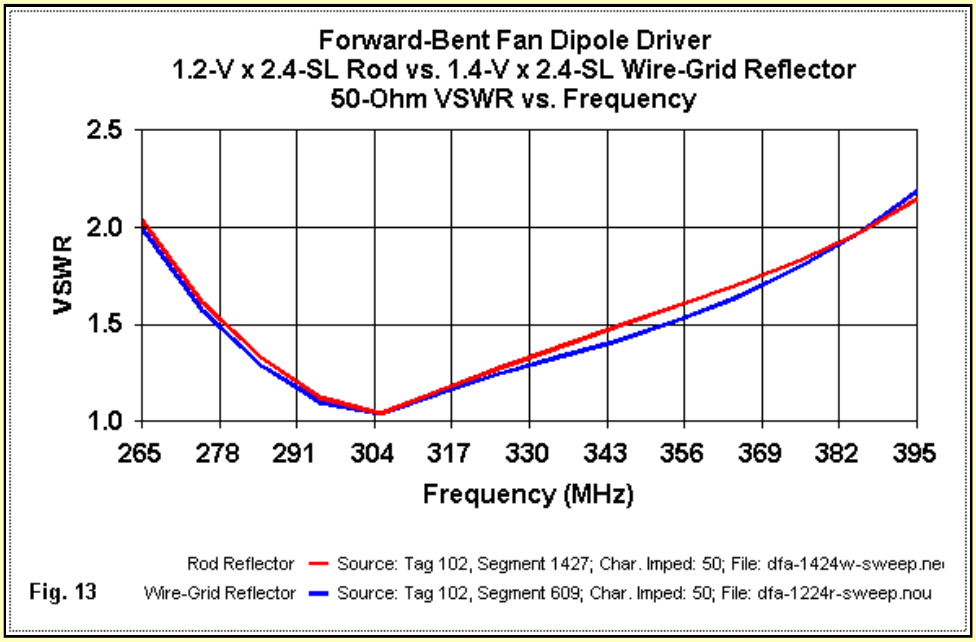

Fig. 13

Fig. 13 compares the 50-Ohm SWR curves for the new wire-grid model and for the large rod reflector that we have just reviewed. Any differences fall in the region of the subtle. At most, the wire-grid curve is displaced upward in frequency by under 1 MHz. There is a slight difference in curve shape in the area where the rod reflector rod lengths are near 1.4 wavelengths. In that area, the rod reflector shows a lower SWR value. However, at the upper end of the passband, the rod-reflector curve becomes steeper than the curve for the wire grid model, suggesting that the wire-grid version would sustain an SWR value below 3:1 for a greater frequency span than the rod version of the array.

With narrow-band corner arrays, we noted that wire-grid models showed a peak gain that is slightly less than the peak gain available from a rod reflector with a 1.4-wavelength vertical dimension, due to the absence of a parasitic effect. We shall encounter the same phenomenon when examining the gain curves for the two arrays in **Fig. 14**.

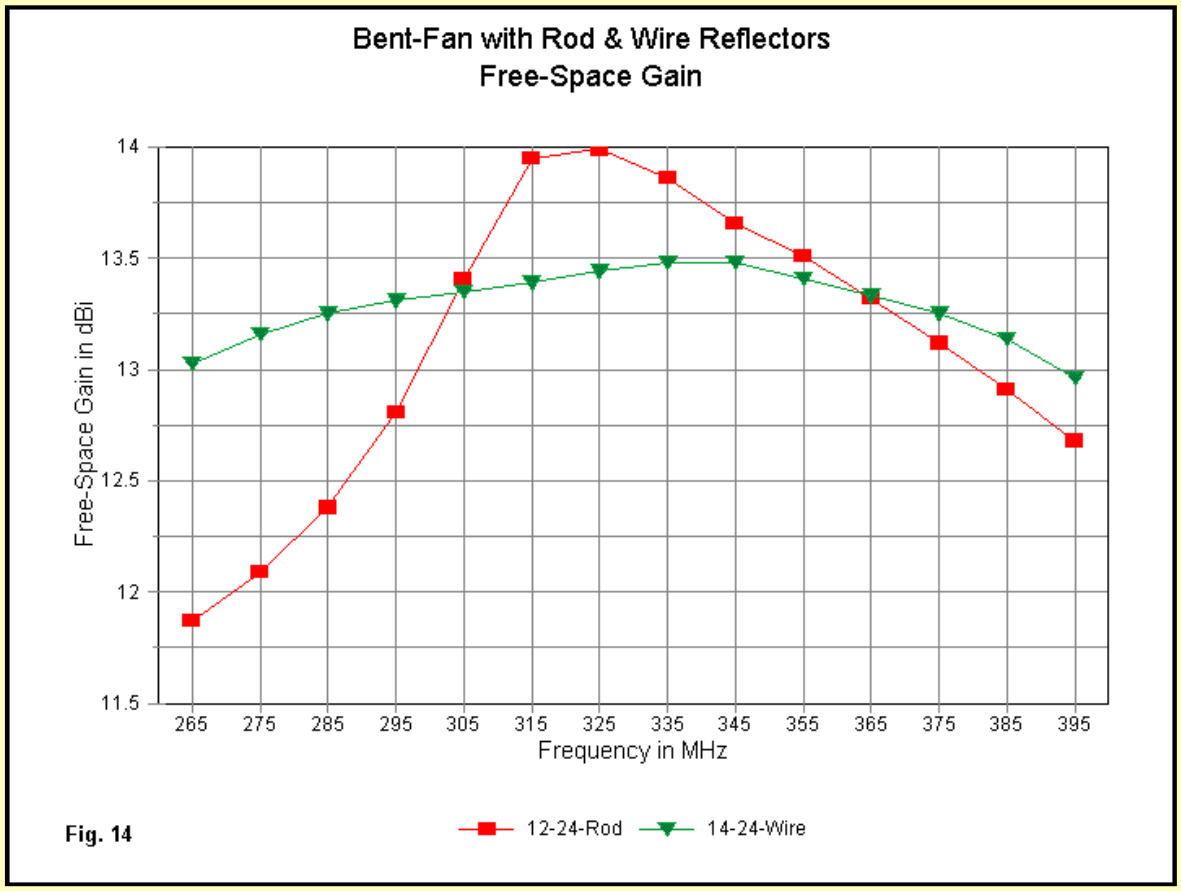

Fig. 14

Peak free-space gain for the wire-grid model is about 13.48 dBi and occurs between 335 and 345 MHz, where the vertical dimension of the reflector is close to 1.6 wavelengths. These values are consistent with earlier results for narrower-band arrays using simply dipole drivers. At these frequencies, the side length is about 2.7 wavelengths. Quite clearly the peak gain of the rod reflector is noticeably higher. However, the rod reflector gain differential across the scanned passband is over 2 dB. The wire-grid model shows a gain differential of only 0.52 dB, and this differential includes the band-edge values that fall slightly outside the 2:1 SWR passband.

The E-plane -3-dB beamwidth of the wire-grid version has a much narrower range of values than for the rod reflector. The beamwidth falls between 46 degrees at 265 MHz and 40 degrees in the 350-MHz region, followed by a gradual increase back to 46 degrees at the top of the SWR passband. However, by the time we reach the end of the scanned range, about 8 MHz higher than the end of the SWR range, the beamwidth increases to 54 degrees. The rod reflector starts with a wider beamwidth at the low end of the passband--54 degrees--and ends at 58 degrees at 395 MHz. The minimum value is 40 degrees at 315 MHz. The changes in beamwidth create an inverse curve relative to the gain values, with a sharp peak near the high-gain frequency. In contrast, the wire-grid model produces a shallow inverse of the equally shallow wire-grid gain curve.

In contrast, H-plane curves coincide more closely with the front-to-back curves, when we smooth the latter to remove the peaks and valleys that appear when using 180-degree values. Both the rod and the wire-grid reflectors show a gradual shrinkage of the beamwidth by 8 degrees across the scanned frequency range. However, the rod reflector range goes from 36 down to 28 degrees, with a small dip in the vicinity of the frequency of highest gain. The wire-grid version ranges from 32 degrees down to 24 degrees, with no discernable dip.

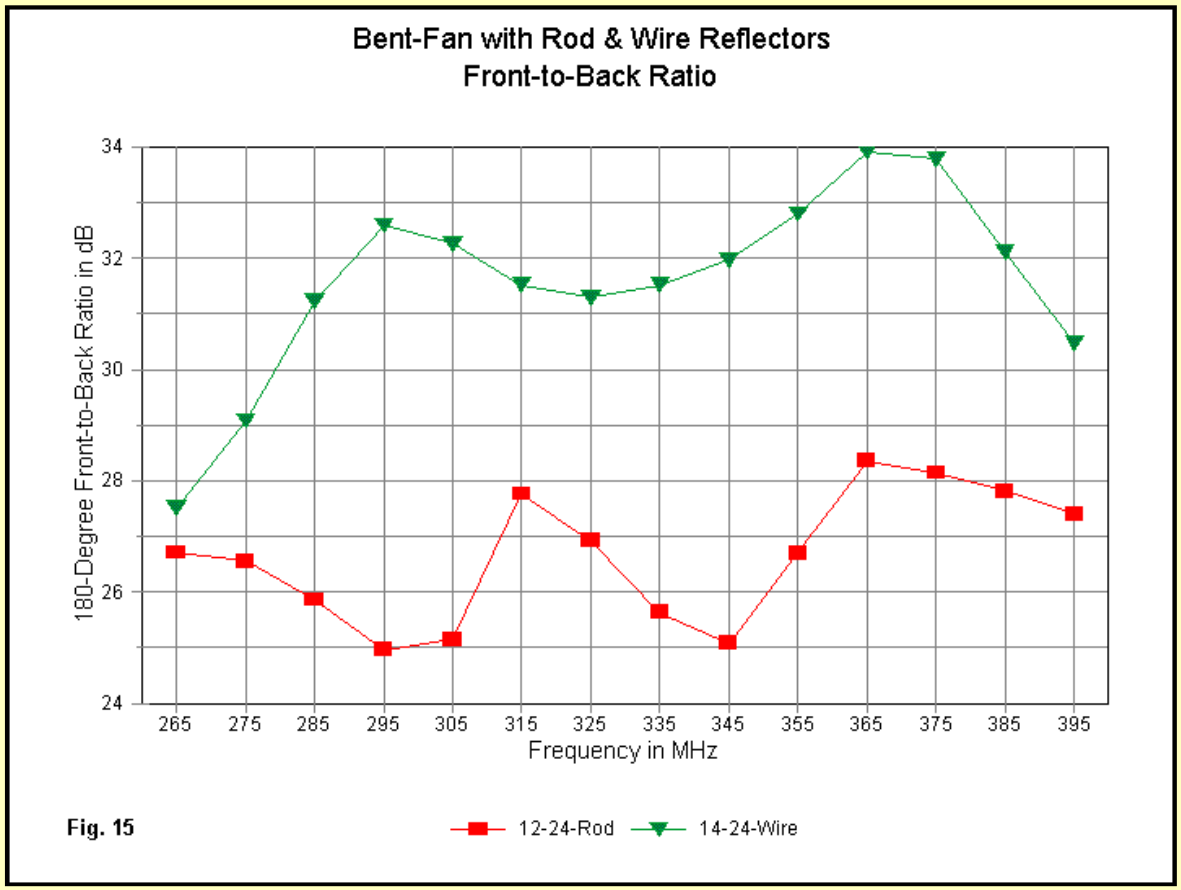

Fig. 15

The advantage in front-to-back ratio of the wire-grid reflector over the rod reflector shows itself very clearly in **Fig. 15**. The wire-grid values show an ascending curve well into the upper third of the passband. However, in the area of 385 MHz, the vertical dimension is about 1.8 wavelengths and the side length has grown to more than 3 wavelengths. As we saw when scanning the large collection of narrow-band arrays, these are values marking the point where continued reflector growth becomes self-defeating.

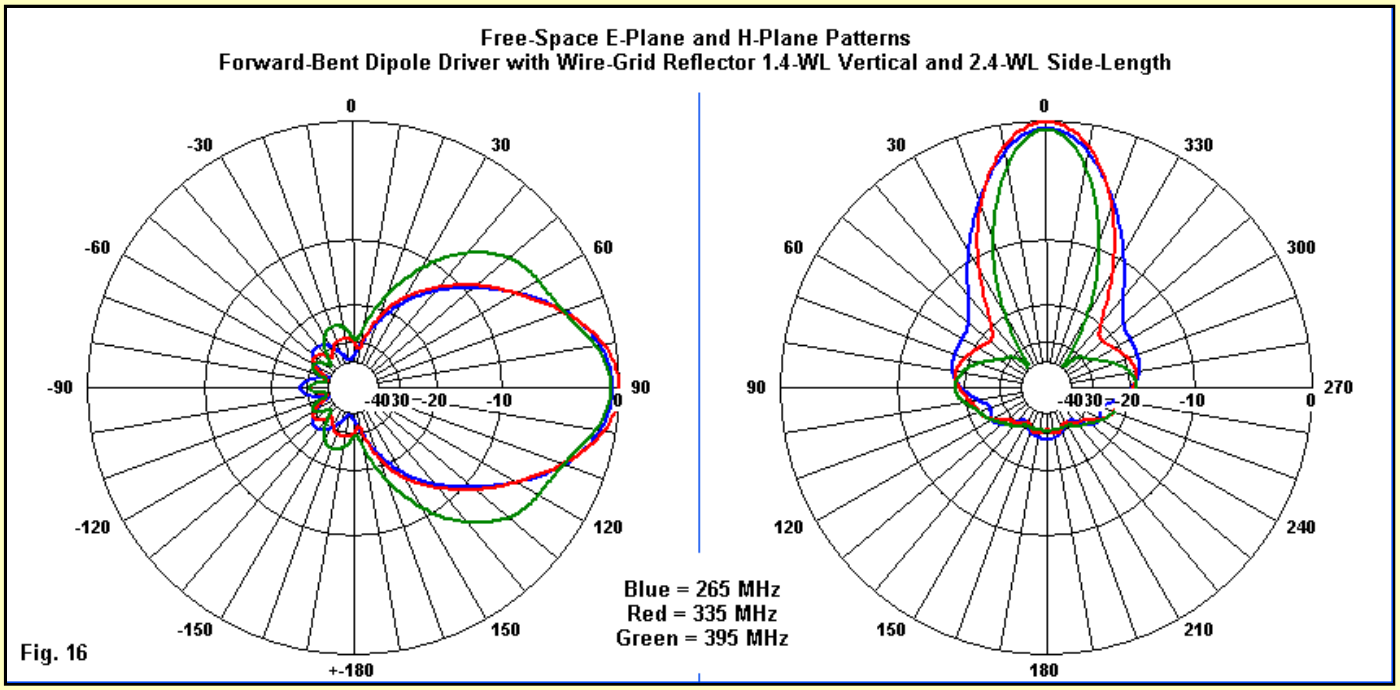

Fig. 16

The sample overlaid patterns in **Fig. 16** provide a glimpse at potential performance of the wire-grid version of the enlarged forward-bent fan dipole driver array. The tighter limits of gain variation show up in both the E-plane and the H-plane patterns. The E-plane patterns show a worst-case front-to-back ratio that is consistently in the 24-26 dB range, despite the use of the bent fan driver. The green line marking the pattern for the array at 8 MHz above the 2:1 SWR passband limit shows clear signs of degradation from the perspective of a clean single-lobe pattern. The increase in beamwidth that we have seen with previous wide-band patterns at the upper end of the range begins to bulge in development of what will become distinct forward side lobes, similar to those one derives from arrays using extended double Zepp (1.25-wavelength) elements. At 395 MHz, we are still a considerable ways from the appearance of such distinct side lobes, but

they show as incipient (or, dare I say it, pregnant) bulges. In contrast, the H-plane patterns are completely normal relative to those we have viewed for the rod reflectors in this series.

To avoid the upper-frequency E-plane pattern distortion, you may select a slightly smaller vertical dimension for the wire-grid reflector. A similar reflector using a 1.2-wavelength vertical dimension and 2.4-wavelength side lengths produces a cleaner--less bulgy--E-plane pattern at the upper end of the scanned range with no change in the SWR curve. The cost is slightly less gain across the passband--about 0.25 to 0.5 dB, depending on the frequency. As well, the front-to-back ratio is also slightly lower. However, the E-plane beamwidth changes by only 4 degrees across the entire frequency range scanned. Wherever pattern shape carries a high weight in the specifications for a wide-band antenna, the 1.2-wavelength vertical solid or screened reflector may be a good choice.

The wire-grid reflector model is more likely to fit applications of very-wire-band applications of the corner array above 1 GHz. Hence, it has been useful to see in what ways solid surface or closely spaced screens will show differing performance curves from rod reflectors. One of the emergent sub-themes of these studies has been the differing behaviors of the two types of corner reflectors. Applying a very-wide-band driver to the corner reflector has both extended our understanding and confirmed earlier conclusions regarding these differences.

One Has to End Somewhere

The study of corner reflectors--even a modeling study using the techniques of this series or improved techniques--does not end here. However, for the level of general guidance and proof of principle, we should end at this point. Further work would not so much uncover added design principles as it would refine them. For many, the further work would be simply more of the same, while for a few, with task-driven design interests, the work would become too specific for general guidance.

However, I hope that these studies do contribute in a small way to the understanding of corner reflectors, including the 180-degree version that I have dubbed the planar reflector. The design has untapped potential in 21st century applications. It is relatively simple to build and adjust, compared to other designs requiring finicky pruning of every element. In the UHF range, especially above 1 GHz, one can build arrays that are both sturdy and adjustable using essentially hardware store components. Moreover, for a very small investment in materials, we acquire a field ripe for endless experimentation.

Whether oriented vertically for FM and similar services or aimed horizontally for point-to-point communications, the corner array likely deserves more than the archival treatment that it has received in the last two decades. Hopefully, these notes make a contribution to its revival.

Go to Main Index